

New Numerical Strategy to Evaluate the Collision Integral of the Boltzmann Equation

Zhiqiang Tan,* Yih-Kanq Chen,† Philip L. Varghese,‡ and John R. Howell§

The University of Texas at Austin, Austin, Texas

Abstract

A new scheme for the calculation of the collision integral of the nonlinear Boltzmann kinetic equation is presented, based on a piecewise constant discrete approximation of the distribution function in phase space and corresponding precalculated collision rate coefficients. The computing effort required for evaluation of the fivefold collision integral is significantly reduced by the use of precalculated rate coefficients. The method was combined with the conservative splitting method to solve the Boltzmann equation for a number of test cases to examine the performance of this method and demonstrate its efficiency.

I. Introduction

The Boltzmann equation, the basic equation of kinetic theory, is required for detailed characterization of gas flows that are far from local thermal equilibrium. Direct numerical solution of the Boltzmann equation presents several computational difficulties. These difficulties arise from the nonlinearity and complexity of the collisional integral, together with the multidimensionality of the equation.

Groups led by Yen and Cheremisin have spearheaded the development of direct numerical solutions of the Boltzmann equation.¹⁻⁵ The basic approaches of the two groups are similar and consist of two steps: 1) evaluation of the collision integral by conducting Monte Carlo simulations (random quadrature), and 2) approximation of the differential operators by the finite-difference method. For the second step, Aristov and Cheremisin's conservative splitting method⁴ is the best currently available because it guarantees conservation of mass, momentum, and energy at every iteration. The Monte Carlo method for computing the collision integral developed by Nordsieck⁶ has been systematically tested and refined for several years. The calculations are time-consuming because a large number of multifold integrations must be performed at every position, velocity, and time grid. The discrete velocity approach has also been studied,⁷ but it does not provide quantitative predictions. Because the collision integral cannot be calculated efficiently, difficult problems involving high Mach numbers, small Knudsen numbers, large derivatives in the flow parameters, and multidimensional physical space cannot be solved within a reasonably short period of time, even on the fastest supercomputer.

In this paper, a new method for evaluating the nonlinear collision integral of the Boltzmann equation is presented. In Sec. 2, the formulation and corresponding numerical method for evaluating the integral are given. It is shown that some basic constants can be computed and stored in advance to reduce total computing time. The important properties of these constants are also discussed. In Sec. 3, the present method, combined with the conservative splitting method,⁴ is applied to one- and two-dimensional cases to examine the method's performance.

FG05-82ER13735

*Graduate student, Department of Mechanical Engineering.

†Postdoctoral Research Associate, Department of Mechanical Engineering.

‡Associate Professor, Department of Mechanical Engineering.

§Professor, Department of Mechanical Engineering.

MASTER

DISCLAIMER

This report was prepared as an account of work sponsored by an agency of the United States Government. Neither the United States Government nor any agency thereof, nor any of their employees, makes any warranty, express or implied, or assumes any legal liability or responsibility for the accuracy, completeness, or usefulness of any information, apparatus, product, or process disclosed, or represents that its use would not infringe privately owned rights. Reference herein to any specific commercial product, process, or service by trade name, trademark, manufacturer, or otherwise does not necessarily constitute or imply its endorsement, recommendation, or favoring by the United States Government or any agency thereof. The views and opinions of authors expressed herein do not necessarily state or reflect those of the United States Government or any agency thereof.

DISCLAIMER

Portions of this document may be illegible in electronic image products. Images are produced from the best available original document.

II. Formulation

Consider the Boltzmann equation without external forces:

$$\frac{\partial f}{\partial t} + \xi \cdot \frac{\partial f}{\partial \mathbf{x}} = \int_0^{4\pi} \int_{-\infty}^{\infty} (f' f_1 - f f_1) G(|\zeta - \xi|, \mathbf{n}) d\zeta d\Omega \quad (1)$$

The position vector \mathbf{x} has the Cartesian components (x, y, z), the velocity vector ξ (or ζ) has corresponding components (ξ_x, ξ_y, ξ_z), f is the velocity distribution function of the gas molecules normalized to the local gas density, Ω is the solid angle, and $\mathbf{n} = (n_x, n_y, n_z)$ is the unit direction vector along the apse line in the plane of the collision. The function $G(g, \mathbf{n}) = g\sigma(g, \mathbf{n})$, where $g = |\zeta - \xi|$ is the relative speed of the collision pair and σ the differential collision cross section, is determined by the form of the intermolecular potential. Subscript 1 indicates quantities for the collision partner, primed quantities indicate values after a collision, and the functional dependence of the distribution functions has been suppressed for compactness, i.e., $f = f(t, \mathbf{x}, \xi)$, $f_1 = f(t, \mathbf{x}, \zeta)$, etc. The velocities of the collision partners after a collision that results in a particular scattering can be determined from

$$\xi' = \xi - \mathbf{n} \mathbf{n} \cdot (\xi - \zeta) \quad (2a)$$

$$\zeta' = \zeta - \mathbf{n} \mathbf{n} \cdot (\zeta - \xi) \quad (2b)$$

The collision integral I in the Boltzmann equation can be separated into two parts:

$$I = A - Bf$$

where

$$A = \int_0^{4\pi} \int_{-\infty}^{\infty} f' f_1 G(g, \mathbf{n}) d\zeta d\Omega$$

and

$$B = \int_0^{4\pi} \int_{-\infty}^{\infty} f_1 G(g, \mathbf{n}) d\zeta d\Omega$$

In order to solve the equation numerically, we may approximate the infinite velocity space by a finite cube $|\xi_i| < V$ (where V is a given constant, $i = x, y, z$) and then divide this cube into smaller cubic elements e_i ($i = 1, \dots, N_e$, where N_e is the total number of elements) of the same side length ΔV . Each velocity axis is divided into an odd number of elements so that the origin is at the center of one of the elements.

The velocity distribution function is discretized by setting

$$f(t, \mathbf{x}, \xi) = \sum_{i=1}^{N_v} \phi_i(\xi) f_i \quad (3)$$

where $f_i \equiv f(t, \mathbf{x}, \xi_i)$, ξ_i are the discretized points in ξ space, N_v is the total number of ξ_i , and ϕ_i is an interpolating function. For simplicity, ϕ_i is chosen as a piecewise constant function in this paper, so that the number of elements N_e is equal to the number of discrete velocity points N_v :

$$N_e = N_v \equiv N$$

Substituting Eq. (3) into (1) and letting $\xi = \xi_k$ yields

$$\frac{\partial f_k}{\partial t} + \xi_k \cdot \frac{\partial f_k}{\partial \mathbf{x}} = A_k - B_k f_k \quad (4)$$

where

$$A_k = \sum_{i=1}^N \sum_{j=1}^N \alpha_{ij}^k f_i f_j, \quad B_k = \sum_{i=1}^N \beta_i^k f_i \quad (5)$$

with *collisional rate coefficients* α_{ij}^k and β_i^k defined by

$$\alpha_{ij}^k = \int_0^{4\pi} d\Omega \int_{-\infty}^{\infty} \phi_i(\xi_k - \mathbf{n} \cdot \mathbf{n} \cdot (\xi_k - \zeta)) \phi_j(\zeta - \mathbf{n} \cdot \mathbf{n} \cdot (\zeta - \xi_k)) G(|\zeta - \xi_k|, \mathbf{n}) d\zeta \quad (6a)$$

$$\beta_i^k = \int_0^{4\pi} d\Omega \int_{-\infty}^{\infty} \phi_i(\zeta) G(|\zeta - \xi_k|, \mathbf{n}) d\zeta \quad (6b)$$

Because the collisional rate coefficients α_{ij}^k and β_i^k are independent of \mathbf{x} , t , f , and initial and boundary conditions, they can be computed and stored in advance for later use on a variety of problems with different geometries or conditions. The collision rate coefficients depend on the collision cross section and hence vary for different gases. For hard-sphere or inverse-power gases, the coefficients are merely rescaled and need not be recalculated.

The limitation of the technique is the large number ($O(N^3)$) of α_{ij}^k and β_i^k to be evaluated and stored. Even when the α_{ij}^k are computed, the $N^2 + N$ multiplications to compute A_k and B_k are extremely time consuming. The key to practical implementation is to exploit some properties of α_{ij}^k that reduce the computing time required. The evaluation of β_i^k is much easier than α_{ij}^k ; the properties of β_i^k are not discussed in detail but are mentioned where appropriate.

The first property of α_{ij}^k is that the coefficient remains unchanged when ξ_i , ξ_j , and ξ_k are shifted (but not rotated) to new positions (say, ξ_i , ξ_m , ξ_n) in velocity space, keeping the relative positions the same. The relation

$$\alpha_{ij}^k = \alpha_{mn}^l$$

follows directly from Eqs. (4) and (6a) because only the relative velocity affects the solution of the Boltzmann equation. Hence, one need only compute α_{ij}^k with $\xi_k = 0$, and the collision rate coefficients for all other k are obtained by shifting. Thus, there are N^2 independent α_{ij}^k ; hereafter, only the computation of $\alpha_{ij}^k|_{\xi_k=0} = \alpha_{ij}$ will be considered. Similarly, $\beta_i^k|_{\xi_k=0} = \beta_i$, and only N coefficients need be computed and stored.

Second, if the angular integral in 4π space is approximated by an M -point numerical integration formula

$$\int_0^{4\pi} F(\mathbf{n}) d\Omega = \sum_{t=1}^M w_t F(\mathbf{n}^t) \quad (7)$$

where w_t are the integration weights and \mathbf{n}^t the integration points, then the number of nonzero α_{ij} is at most $9MN$. The proof for this property can be outlined as follows. If $\alpha_{ij} \neq 0$ for some i and j , then, with $\xi_k = 0$, Eq. (6a) gives vector inequalities

$$|\xi_i - \mathbf{n} \cdot \zeta| < (\Delta V/2)\mathbf{i}$$

$$|(\mathbf{I} - \mathbf{n} \cdot \mathbf{n}) \cdot \zeta - \xi_j| < (\Delta V/2)\mathbf{i} \quad (8)$$

where \mathbf{I} is the unit matrix, \mathbf{i} is the unit vector, and the vector magnitude of a vector $|\mathbf{v}| = (|v_x|, |v_y|, |v_z|)$. To satisfy these two inequalities, the following must hold:

$$|(\xi_i \times \mathbf{n}^t)_r| < (S^t - |n_r^t|) \frac{\Delta V}{2}, \quad i = 1, \dots, N, \quad t = 1, \dots, M, \quad r = x, y, z \quad (9a)$$

$$|\xi_j \cdot \mathbf{n}^t| < S^t \frac{\Delta V}{2}, \quad j = 1, \dots, N, \quad t = 1, \dots, M \quad (9b)$$

where $S^t = |n_1^t| + |n_2^t| + |n_3^t|$, and subscript r on the left side of Eq. (9a) denotes the r th component of a vector. Inequality (9a) represents a hexagon in velocity space. The maximum number of ξ_i in the hexagon is less than $3N^{1/3}$ and this occurs when $|n_x^t| = |n_y^t| = |n_z^t| = 1/\sqrt{3}$. Inequality (9b) represents a plate of thickness $S^t \Delta V$. The maximum number ξ_j that lie in this plate is less than $3N^{2/3}$, and this is obtained when $|n_x^t| = |n_y^t| = |n_z^t|/\sqrt{2} = 1/2$ (or any permutation of subscripts x, y, z). Therefore, the total number of pairs (ξ_i, ξ_j) ($i, j = 1, \dots, N$) that satisfy Eqs. (9a) and (9b) does not exceed $9N$ for any \mathbf{n}^t . Because there are M vectors \mathbf{n}^t , the maximum number of nonzero α_{ij} is $9MN$. Numerical experiments were conducted to verify this for N ranging from 3^3 to 11^3 , and the number of nonzero was found to be between $0.9MN$ and $2.1MN$. The exact number depended on the discretization of velocity space and the choice of numerical scheme for angular integration. Because $M \ll N$ typically, this property greatly reduces the number of nonzero α_{ij} .

Combining Eqs. (6a) and (7), the five-dimensional integrals α_{ij} may be written explicitly as

$$\alpha_{ij} = \sum_{t=1}^M w_t \int_{-\infty}^{\infty} \phi_i(\mathbf{n}^t \cdot \mathbf{n}^t \cdot \zeta) \phi_j(\zeta - \mathbf{n}^t \cdot \mathbf{n}^t \cdot \zeta) G(|\zeta|, \mathbf{n}^t) d\zeta \quad (10)$$

It is convenient to transform variables to permit evaluation of the integral by Gaussian quadrature. The following transformation was used:

$$\eta = \begin{pmatrix} \eta_x \\ \eta_y \\ \eta_z \end{pmatrix} = \begin{pmatrix} n_x & n_y & n_z \\ -n_x n_y & 1 - n_y^2 & -n_y n_z \\ -n_x n_z & -n_y n_z & 1 - n_z^2 \end{pmatrix} \begin{pmatrix} \xi_x \\ \xi_y \\ \xi_z \end{pmatrix} = R \xi$$

For convenience, it is assumed that the M points chosen for the angular integration are such that all n_r^t are nonzero in Eq. (7). (If any one of the components n_r^t is zero, the integration points can be rotated to new sets so that all n_r^t are nonzero. This does not change the order of accuracy of numerical integration because of the spherical symmetry of the domain of the integral.) It is easy to show that $|R| = n_x$ ($| \cdot |$ denotes the determinant) and that the inverse of R exists. Substituting in Eq. (10)

$$\alpha_{ij} = \sum_{t=1}^M w_t \int_{a_3}^{b_3} d\eta_z \int_{a_2}^{b_2} d\eta_y \int_{a_1}^{b_1} G(|R^{-1}\eta|, \mathbf{n}^t) \frac{d\eta_x}{|n_x^t|} \quad (11)$$

where

$$\begin{aligned}
 a_1 &= \max_s \left(\frac{(\xi_j)_s}{n_s^t} - \frac{\Delta V}{2|n_s^t|} \right), \quad b_1 = \min_s \left(\frac{(\xi_j)_s}{n_s^t} + \frac{\Delta V}{2|n_s^t|} \right), \\
 &\quad s = x, y, z \\
 a_2 &= (\xi_j)_y - \frac{\Delta V}{2}, \quad b_2 = (\xi_j)_y + \frac{\Delta V}{2} \\
 a_3 &= \max \left((\xi_j)_z - \frac{\Delta V}{2}, -\frac{n_x^t(\xi_j)_x + n_y^t(\xi_j)_y}{n_z^t} - \frac{|n_x^t| \Delta V}{2|n_z^t|} \right) \\
 b_3 &= \min \left((\xi_j)_z + \frac{\Delta V}{2}, -\frac{n_x^t(\xi_j)_x + n_y^t(\xi_j)_y}{n_z^t} + \frac{|n_x^t| \Delta V}{2|n_z^t|} \right)
 \end{aligned}$$

and the integral is set to zero if $b_r \leq a_r$ for any r ($r = 1, 2$, and 3). Here $(\xi_j)_s$ denotes the s th component of ξ_j .

Thus, the total number of independent nonzero collisional rate coefficients α_{ij}^k is of the order of MN instead of N^3 . This reduction is very important because it determines the computation time and memory size required for data storage. The coefficients can be stored efficiently using one array to store the values of the nonzero elements and another to store the indices of these elements. When a flow is computed, the collision integral may be evaluated rapidly and efficiently using the stored collision rate coefficients α and β . In contrast, the Monte Carlo technique is relatively inefficient because it requires repeated random number generations, location of ζ' and ζ , and evaluation of G .

III. Numerical Examples

The technique was applied to solve the Boltzmann equation for three cases to demonstrate its capabilities. In these calculations, velocity space was approximated by a cube of side $4\sqrt{3}v_0$, where $v_0 = (kT_0/m)^{1/2}$ is a characteristic molecular velocity in the unperturbed gas. Each side of this domain was divided into 5, giving 125 small cubic elements in velocity space. The shifting property of the collision rate coefficient was utilized to consider collisions between molecules near the edges of the cube with partners outside this region, so that depleting collisions were computed on an enlarged domain ($9 \times 9 \times 9$). An $M = 18$ point formula for the angular integral was used in the numerical integrations. For simplicity, the gas molecules were modeled as hard spheres. The computed α and β were stored and used for all three problems. The discretized Boltzmann equation was solved using the conservative splitting method.⁴ Steady-state problems were solved by an explicit transient approach.

Stationary Shock Wave

Figure 1 presents a comparison between the results obtained using the present method (solid line) and those of Aristov and Cheremisin⁴ (symbols) for the structure of a stationary one-dimensional shock wave in a hard-sphere gas flow at Mach 2.5. The reduced density N , velocity U , and temperature T are plotted vs nondimensional distance X . Reduced quantities are defined by

$$N = \frac{N_x - N_0}{N_1 - N_0}, \quad U = \frac{U_x - U_0}{U_1 - U_0}, \quad T = \frac{T_x - T_0}{T_1 - T_0}$$

where subscripts 0 and 1 denote upstream and downstream values, respectively. Distances have been scaled by the mean free path $\lambda (= 1/\sqrt{2\pi d^2 N_0})$ in the unshocked gas. The predictions of the two techniques are in very good agreement.

Piston Problem

The technique was then applied to a transient problem presented by Aristov and Cheremisin.⁴ The half-space, $x > 0$, is filled with gas at uniform temperature and density T_0 and N_0 , respectively, moving with uniform mean velocity $2v_0$ in the negative x direction. The molecular velocity distribution is Maxwellian when $t < 0$. At the instant $t = 0$, an infinite wall perpendicular to the x axis is placed at $x = 0$. The reflection of gas molecules on the wall is assumed to be specular.

The semi-infinite physical space was replaced by the finite segment $[0, L]$. The following characteristic parameters are used for nondimensionalization:

$$x^* = \frac{L}{30}, \quad t^* = \frac{L}{3\sqrt{2}v_0}, \quad f^* = \frac{N_0}{(2\pi)^{3/2}v_0^3}, \quad \xi^* = \sqrt{2}v_0 t, \quad Kn = \frac{\lambda}{x}$$

The only characteristic length in the problem is the shock-wave thickness, which is not known a priori, so that the choice of x^* and t^* is rather arbitrary. In Fig. 2, the dimensionless density and temperature profiles at various dimensionless times are presented for $Kn = 0.02$. Corresponding results for $Kn = 0.2$ are presented in Fig. 3. The results show that a sharp gradient propagates in the positive x direction corresponding to the formation of a shock because of collisions between the reflected and incident molecules. Comparing the results of the two cases, the shock thickness is seen to be inversely related to the Knudsen number (as expected) and is approximately $4x^*$ at $Kn = 0.02$ and $12x^*$ at $Kn = 0.2$. At the lower Knudsen number, the shockwave profile rapidly approaches steady state and moves at constant speed thereafter. Steady-state propagation is delayed at the higher Knudsen number. Local departures from equilibrium are most clearly seen in the temperature profile because it is the highest moment of the distribution function. The maximum in the temperature profiles at early times, which is very pronounced at the higher Knudsen number, corresponds to the fact that reflected molecules traveling at $2v_0$ penetrate some distance into the incoming gas before being thermalized by collisions. Similar trends are seen in the results of Aristov and Cheremisin⁴ obtained by Monte Carlo evaluation of the collision integral. It should also be noted that these solutions were obtained in collision-dominated flows (low Knudsen numbers) where Boltzmann equation solutions have traditionally been difficult because of computational difficulty in evaluating the collision term to satisfactory precision.

Figure 4 shows the effect of Kn on the flowfield at nondimensional time $t = 10$. For negligible collision rates ($Kn \rightarrow \infty$), the reflected molecules propagate freely without interacting with incoming molecules to thermalize the kinetic energy. This leads to a lower temperature in the vicinity of the wall and a wide transition region between the zone of unperturbed gas and gas that has been brought to rest by the wall. Note that when collisions are relatively unimportant ($Kn = 2$), the profiles appear slightly distorted. The distortion arises because the division of velocity space into 125 elements is insufficient to describe the convection term in the Boltzmann equation. For collisionless flow ($Kn \rightarrow \infty$), the distortions were somewhat larger for the same discretization. These distorted results are not shown in Fig. 4, and the results for collisionless flows were calculated using a denser grid of $13 \times 13 \times 13$ for the convective and unsteady terms with the collision integral set to zero. As Kn decreases, the distortions disappear, indicating that the division into 125 elements is sufficient for accurate calculation of the collision integral.

A remedy for the distortion problem at large Kn may be to use a different number of velocity space divisions for the left- and right-hand sides of the Boltzmann equation. A small number of A_k (say, 125, as in this example) may be calculated and then interpolated to denser velocity nodes for the convective term of the Boltzmann equation.

Comparisons were also made between conservative and nonconservative solutions to this problem. The computations indicated that the present method required the conservative scheme for satisfactory solutions using the fairly coarse grid chosen in velocity space. The nonconservative results obtained were considerably better than those obtained by Monte Carlo evaluation of the collision integral.⁴

Two-Dimensional Flow

The steady flow of a rarefied gas over a finite flat plate was also solved using the new technique. Similar problems have been studied by Cheremisin using Monte Carlo evaluation of the collision integral.^{8,9} In this test case, the wall accommodation coefficient was taken to be 0.5 and the wall temperature was set to the temperature of the unperturbed flow. The Mach number of the incident flow was set at 2, and the length of the plate was twice the mean free path in the unperturbed flow, giving a Knudsen number of 0.5. The physical space was divided into 260 unequal cells. Figure 5 presents the density contours in the flowfield. The locus of points of maximum density may be identified with an oblique shock, which appears to intersect the plate about 0.3λ behind the leading edge and extends at an angle of approximately 65 degree to the plate. (It should be noted that the scale in the figure has been stretched in the y direction for clarity.) These steady-state results are in qualitative agreement with Cheremisin's result⁸ for a higher-speed flow ($M = 4$). The present calculations were run at conditions that matched his earlier paper,⁹ but the results do not agree.

Figure 6 is a plot of density, mean x velocity, and temperature along the plane $y = 0$; the plate extends from 0 to 2. The density and temperature are increased just upstream (one or two mean free paths) of the plate and decline steadily over the length of the plate. The velocity drops sharply just upstream of the plate, declines slowly over the leading edge, and is almost constant over the trailing edge. In the wake, the velocity recovers rapidly to the freestream value, but there is a persistent density decrease and corresponding temperature increase relative to the freestream. The trends in density and temperature obtained in these results are similar to those obtained by Cheremisin for Mach 4 flow over heated and cooled plates.⁹ The same trends are also obtained from direct simulation Monte Carlo calculations of higher-speed flows.¹⁰

The present solution technique could not be extended immediately to higher speed flows ($M > 3$) with good accuracy, because the present division of velocity space into five elements in each direction with piecewise constant interpolation cannot represent bimodal distribution functions satisfactorily. A higher-order interpolating function and a finer mesh for the left-hand side terms would produce more accurate results without increasing computing time significantly. Work on these areas is in progress.

IV. Conclusions

A new numerical method to evaluate the collision integral of the Boltzmann equation was presented. The technique was successfully applied to obtain solutions of the Boltzmann equation for some example problems. The following conclusions may be drawn:

- 1) The present method can generate collision integrals efficiently since most of the work needed for numerical integration is done by precalculation. Because the precalculated collision rate coefficients are independent of physical space, the method is readily extended to multidimensional problems. The examples show its ability to deal

with problems with strong collision effects. Good agreement was obtained with results obtained by the Monte Carlo method for the stationary shock-wave problem.

2) The efficiency and accuracy of the present technique may be improved by: using different velocity meshes for convection and collision terms; applying higher order interpolating functions; and using a better quadrature scheme for angular integrations.

Acknowledgement

This research was supported by the U.S. Department of Energy under grant DE-FG05-87ER13735.

References

- ¹Yen, S. M., "Monte Carlo Solutions of Nonlinear Boltzmann Equation for Problems of Heat Transfer in Rarefied Gases," *International Journal of Heat and Mass Transfer*, Vol. 14, 1971, pp. 1865-1869.
- ²Yen, S. M., and Ng, W., "Shock Wave Structure and Inter-molecular Collision Laws," *Journal of Fluid Mechanics*, Vol. 65, 1974, pp. 127-144.
- ³Cheremisin, F. G., "Numerical Methods for the Direct Solution of the Kinetic Boltzmann Equation," *U. S. S. R. Computational Mathematics and Mathematical Physics*, Vol. 25, 1985, pp. 156-166.
- ⁴Aristov, V. V., and Cheremisin, F. G., "The Conservative Splitting Method for Solving Boltzmann's Equation," *U. S. S. R. Computational Mathematics and Mathematical Physics*, Vol. 20, 1980, pp. 208-225.
- ⁵Yen, S. M., and Tcheremissine, F. G., "Monte-Carlo Solution of the Nonlinear Boltzmann Equation," *Progress in Aeronautics and Astronautics: Rarefied Gas Dynamics*, Vol. 74, edited by S. S. Fisher, AIAA, New York, 1981, Pt. I, pp. 287-304.
- ⁶Nordsieck, A., and Hicks, B. L., "Monte Carlo Evaluation of the Boltzmann Collision Integral," *Rarefied Gas Dynamics*, edited by C. L. Brundin, Vol. 1, 1967, pp. 695-710.
- ⁷Cabannes, H., "Couette Flow for a Gas with a Discrete Velocity Distribution," *Journal of Fluid Mechanics*, Vol. 76, 1976, pp. 273-287.
- ⁸Tcheremissine, F. G., "Solution of the Boltzmann Equation for Rarefied Gas Dynamics," *Rarefied Gas Dynamics*, Vol. 1, edited by O. M. Belotserkovskii, M. N. Kogan, S. S. Kutateladze, and A. K. Rebrov, Plenum, New York, pp. 303-310.
- ⁹Cheremisin, F. G., "Solution of the Plane Problem of the Aerodynamics of a Rarefied Gas on the Basis of Boltzmann's Kinetic Equation", *Soviet Physics-Doklady*, Vol. 18, 1973, pp. 203-204.
- ¹⁰Hermina, W. L., "Monte Carlo Simulation of Rarefied Flow Along a Flat Plate," AIAA Paper 87-1547, 1987.

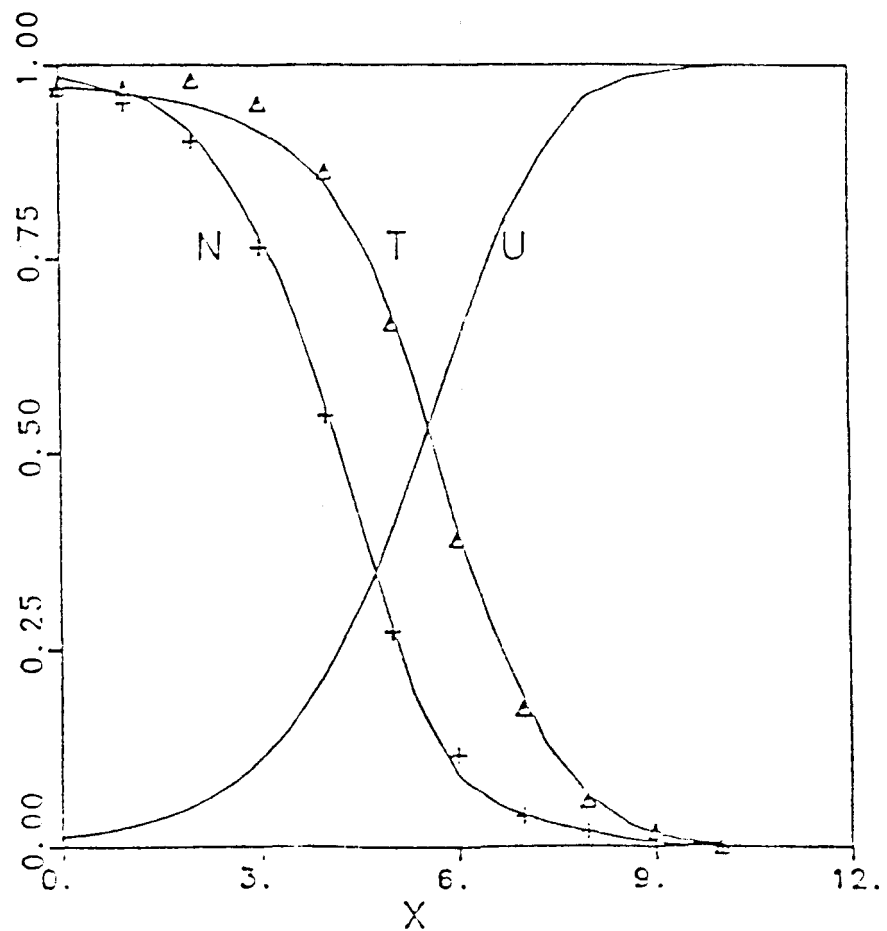


Fig. 1 Structure of a stationary shock wave in a hard-sphere gas at Mach 2.5. The solid lines are the results of this work; the symbols were taken from Aristov and Cheremisin.⁴ N, U, and T denote reduced density, velocity, and temperature, respectively. X has been scaled by the mean free path in the unshocked gas.

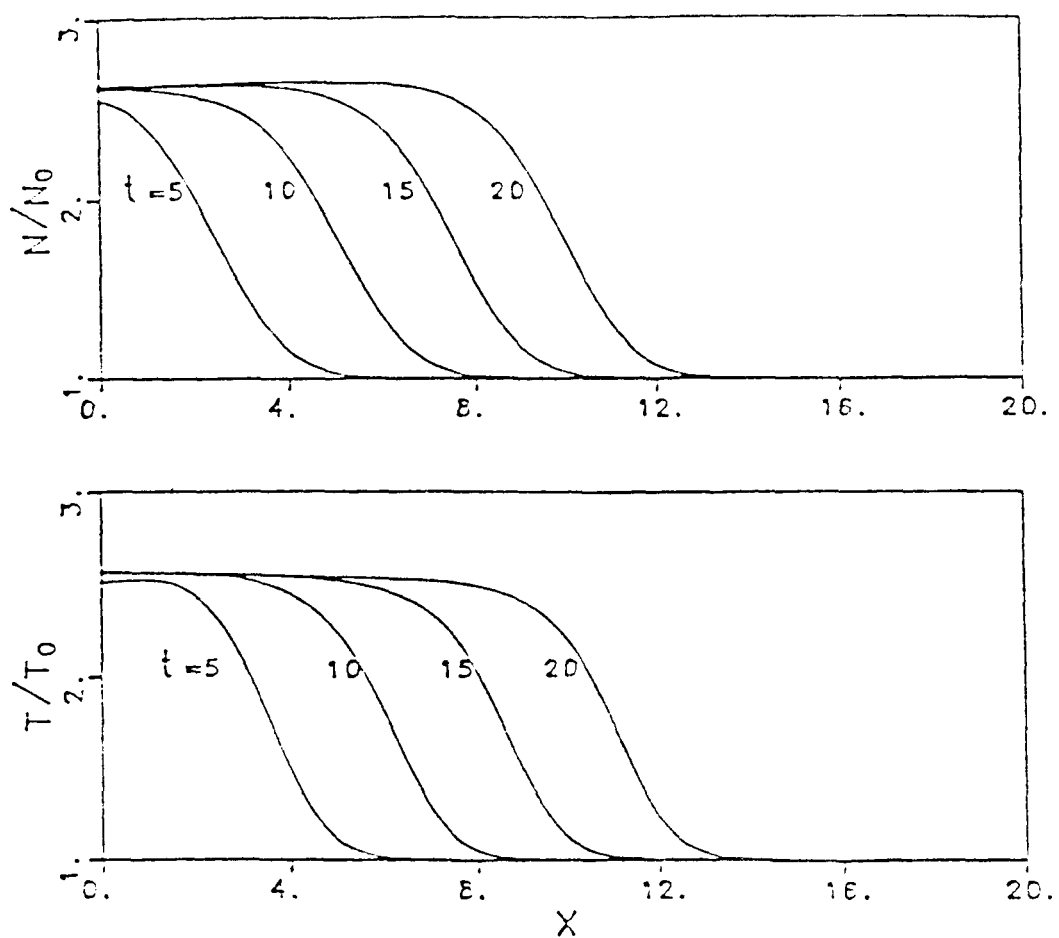


Fig. 2 Nondimensional density and temperature at various times for the reflecting piston problem when $\text{Kn} = 0.02$.

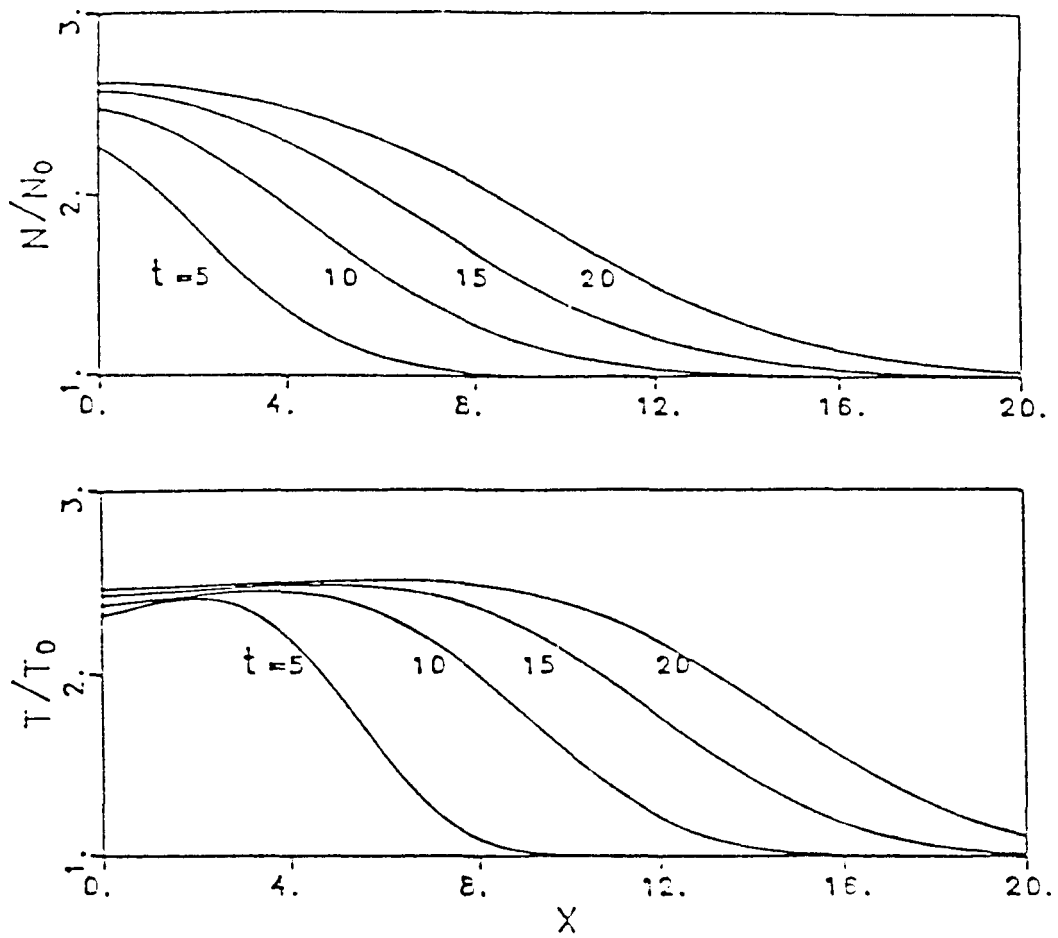


Fig. 3 Nondimensional density and temperature at various times for the reflecting piston problem when $\text{Kn} = 0.2$.

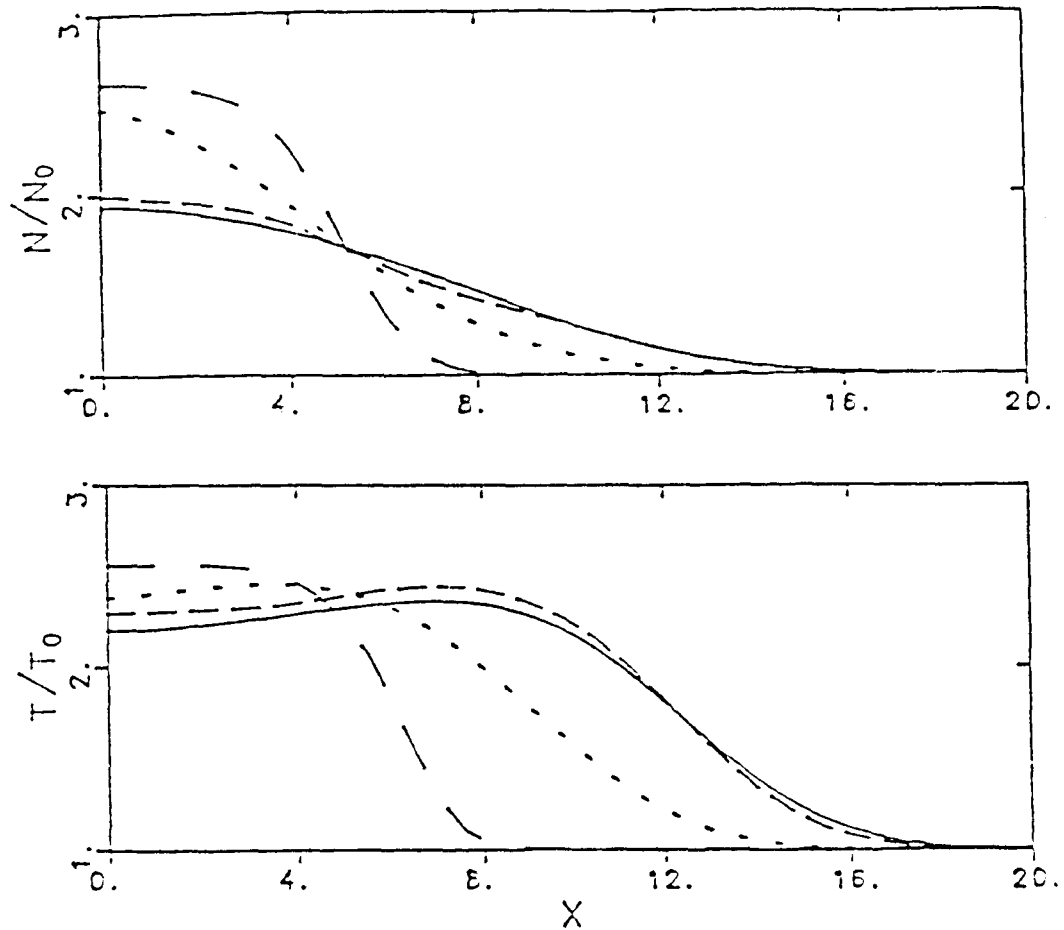


Fig. 4 Effect of Kn on the density and temperature profiles at nondimensional time $t = 10$ for the reflecting piston problem. The collisionless flow ($\text{Kn} = \infty$) was computed with a $13 \times 13 \times 13$ grid in velocity space. All other cases were computed with a $5 \times 5 \times 5$ grid. The distortion of the $\text{Kn} = 2$ case resulting from the coarse velocity grid may be noted. — $\text{Kn} = \infty$; - - - $\text{Kn} = 2$; - - - - $\text{Kn} = 0.2$; - - - - - $\text{Kn} = 0.02$.

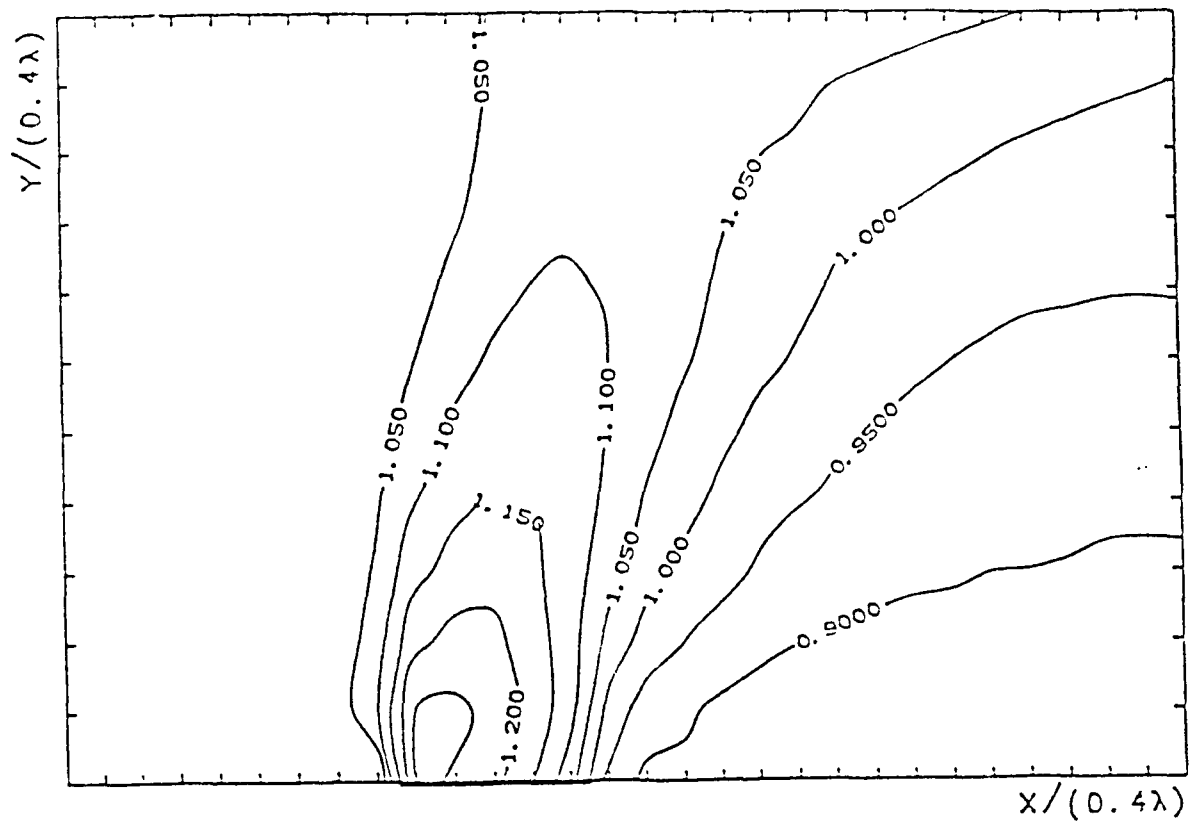


Fig. 5 Density contours calculated for supersonic flow of a monatomic gas over a flat plate. The incident Mach number is 2, and the plate length is 2λ , where λ is the mean free path in the freestream. Gas/surface interactions are modeled by a combination of specular reflection and diffusion, with a wall accommodation coefficient of 0.5; the wall temperature is specified to be the same as the freestream temperature. Distances have been scaled by 0.4λ so that the plate is 5 units long. Note that the y scale has been stretched for clarity. The density has been normalized by the freestream value.

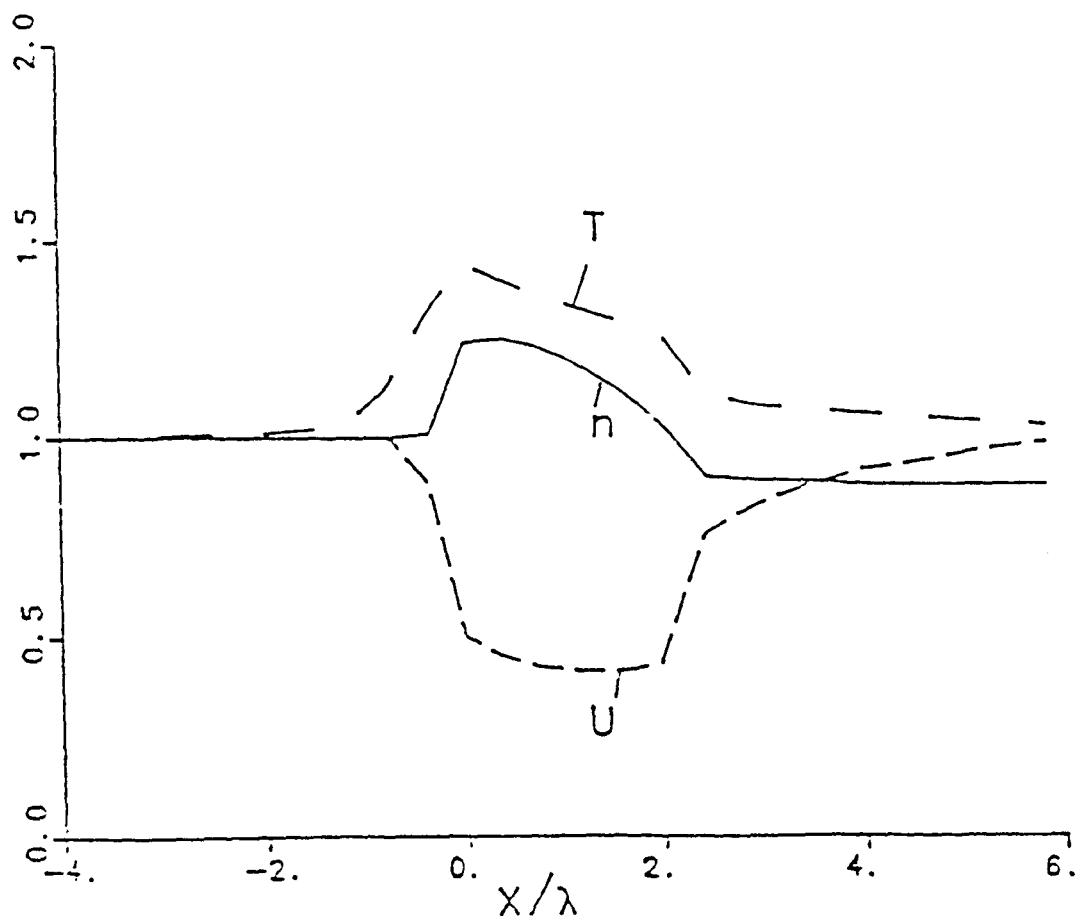


Fig. 6 Variation of density, mean velocity, and temperature along $y = 0$, for flow over a flat plate shown in Fig. 5. The plate extends from $x = 0$ to $x = 2$. All fluid properties have been normalized by the corresponding freestream values.